Clinical Infectious Diseases

MAJOR ARTICLE

Optimal Threshold of Controlled Attenuation Parameter for Detection of HIV-Associated NAFLD With Magnetic Resonance Imaging as the Reference Standard

Veeral H. Ajmera,[1,2] Edward R. Cachay,[3] Christian B. Ramers,[4] Shirin Bassirian,[1] Seema Singh,[1] Richele Bettencourt,[1] Lisa Richards,[1] Gavin Hamilton,[5] Michael Middleton,[5] Katie Fowler,[5] Claude Sirlin,[5] and Rohit Loomba[1,2,6]

[1]NAFLD Research Center, Department of Medicine, University of California, San Diego, La Jolla, California, USA, [2]Division of Gastroenterology, Department of Medicine, University of California, San Diego, La Jolla, California, USA, [3]Division of Infectious Diseases, Owen Clinic, University of California San Diego, San Diego, California, USA, [4]Laura Rodriguez Research Institute, Family Health Centers of San Diego, San Diego, California, USA, [5]Liver Imaging Group, University of California, San Diego, La Jolla, California, USA, and [6] Division of Epidemiology, Department of Family and Preventive Medicine, University of California, San Diego, La Jolla, California, USA

Background. Controlled attenuation parameter (CAP) is an ultrasound-based point-of-care method to quantify liver fat; however, the optimal threshold for CAP to detect pathologic liver fat among persons living with human immunodeficiency virus (HIV; PLWH) is unknown. Therefore, we aimed to identify the diagnostic accuracy and optimal threshold of CAP for the detection of liver-fat among PLWH with magnetic resonance imaging proton-density fat fraction (MRI-PDFF) as the reference standard.

Methods. Patients from a prospective single-center cohort of PLWH at risk for HIV-associated nonalcoholic fatty liver disease (NAFLD) who underwent contemporaneous MRI-PDFF and CAP assessment were included. Subjects with other forms of liver disease including viral hepatitis and excessive alcohol intake were excluded. Receiver operatic characteristic (ROC) curve analysis were performed to identify the optimal threshold for the detection of HIV-associated NAFLD (liver fat ≥ 5%).

Results. Seventy PLWH (90% men) at risk for NAFLD were included. The mean (± standard deviation) age and body mass index were 48.6 (±10.2) years and 30 (± 5.3) kg/m^2, respectively. The prevalence of HIV-associated NAFLD (MRI-PDFF ≥ 5%) was 80%. The M and XL probes were used for 56% and 44% of patients, respectively. The area under the ROC curve of CAP for the detection of MRI-PDFF ≥ 5% was 0.82 (0.69–0.95) at the cut-point of 285 dB/m. The positive predictive value of CAP ≥ 285 dB/m was 93.2% in this cohort with sensitivity of 73% and specificity of 78.6%.

Conclusions. The optimal cut-point of CAP to correctly identify HIV-associated NAFLD was 285 dB/m, is similar to previously published cut-point for primary NAFLD and may be incorporated into routine care to identify patients at risk of HIV-associated NAFLD.

Keywords. NASH; steatosis; MRI-PDFF.

Among persons living with human immunodeficiency virus (HIV; PLWH), liver disease is a leading cause of morbidity and mortality [1]. Historically, coinfection with viral hepatitis B and C were major contributors to liver disease among PLWH, but these risk factors are increasingly controlled with improved antiviral therapy for viral hepatitis. With increases in the long-term survival of PLWH and in the prevalence of metabolic syndrome, which affects approximately 25% of PLWH, HIV-associated nonalcoholic fatty liver disease (NAFLD) is emerging as a major cause of liver disease [2–4].

HIV-associated NAFLD occurs in the presence of metabolic risk factors and in the absence of viral hepatitis and pathologic alcohol use among PLWH. Although primary NAFLD and HIV-associated NAFLD have similar risk factors, multiple unique factors contribute to disease pathogenesis in PLWH including lipodystrophy [5], direct and indirect viral effects, and increased permeability of the gut epithelium [6]. The pathogenic role of antiretroviral therapy in HIV-associated NAFLD remains unclear and include older nucleoside reverse transcriptase inhibitors (NRTIs) causing mitochondrial toxicity, insulin resistance, and impaired fatty acid oxidation contributing to HIV-associated NAFLD [7]. Thus, multiple unique factors contribute to the pathogenesis of HIV-associated NAFLD.

Several noninvasive imaging tests have been evaluated for the detection of liver fat including conventional ultrasound, computed tomography, and magnetic resonance spectroscopy but are limited by low sensitivity [8], ionizing radiation [9], and the requirement for technical expertise [10], respectively. Magnetic resonance imaging proton density fat fraction (MRI-PDFF) is a technique that can be included in conventional MRI exams and is an accurate, reproducible biomarker for the detection of NAFLD and liver fat quantification that has similar accuracy

Received 20 December 2019; editorial decision 30 March 2020; accepted 23 September 2020; published online September 25, 2020.

Correspondence: R. Loomba, ACTRI Bldg, 1W202, 9452 Medical Center Dr, La Jolla, CA 92037 (roloomba@ucsd.edu); http://fattyliver.ucsd.edu.

Clinical Infectious Diseases® 2021;72(12):2124–31

DOI: 10.1093/cid/ciaa429

to magnetic resonance spectroscopy (MRS) and is more widely available [11–19]. Although MRI-PDFF can be considered a useful reference standard for the quantification of liver fat, a low-cost point-of-care test would be ideal to screen a large at-risk population. Controlled attenuation parameter (CAP) is a novel ultrasound-based test to quantify liver fat during a liver stiffness (LS) measurement obtained by vibration-controlled transient elastography (VCTE) known as Fibroscan [20]. Although CAP is less accurate than MRI-PDFF [18], it does allow for a rapid, point-of-care, noninvasive assessment of elevated liver fat (MRI-PDFF ≥ 5%) with good sensitivity and specificity [21]. We hypothesized that the optimal CAP cutoff for HIV-associated NAFLD would be higher than 238 dB/m, which was not derived in patients with NAFLD and was utilized in many studies of HIV-associated NAFLD. The current study aims to evaluate the diagnostic accuracy of CAP for the diagnosis of HIV-associated NAFLD and to identify an optimal disease-specific threshold for detection of elevated liver fat using MRI-PDFF as the reference standard.

MATERIAL AND METHODS

Study Design and Population

This is a cross-sectional study of a prospectively, consecutively recruited cohort of PLWH who are at risk for HIV-associated NAFLD. The study was designed and conducted according to the Standards for Reporting of Diagnostic Accuracy guidelines (Supplemental Table 1). The protocol was Health Insurance Portability and Accountability Act (HIPAA) compliant and was approved by the UCSD Institutional Review Board. Informed written consent was obtained from each participant before study enrollment. Participants were enrolled from the University of California at San Diego (UCSD) primary care clinics and subspecialty clinics including those focused on HIV treatment and liver diseases, and the study was conducted between 1 March 2016 and 1 January 2018, at UCSD NAFLD Research Center.

Inclusion and Exclusion Criteria

Inclusion criteria were as follows: adult patients at least 18 years of age with a history of HIV infection and at least ≥1 of the following risk factors for HIV-associated NAFLD; hypertriglyceridemia (>150 mg/dL), dyslipidemia (low density lipoprotein (LDL) > 160 mg/dL or high density lipoprotein (HDL) < 40 mg/dL), serum ALT above the upper limit of normal (>19 U/L for women and >30 U/L for men), body mass index (BMI) >25 kg/m^2, hyperuricemia, prediabetes or diabetes defined by American Diabetes Association criteria (fasting plasma glucose [FPG] 100–125 or HbA1c 5.7%–6.4% or 2 hour plasma glucose 140–199 after 75 gram glucose tolerance test for prediabetes and FPG ≥ 126 or HbA1c ≥ 6.5% or 2 hour plasma glucose ≥ 200 after 75 gram glucose tolerance test or in a patient with classic symptoms a random plasma glucose ≥200) [22].

Exclusion criteria included serologic testing to exclude the presence of other forms of liver disease and are outlined in the supplemental material. Further exclusion criteria included alcohol intake of more than 30 g/day in the previous 10 years or greater than 10 g/day in the previous year, evidence of cirrhosis based on clinical assessment or imaging, active illicit drug use, pregnancy, evidence of hepatocellular carcinoma, ingestion of drugs known to cause hepatic steatosis, or inability to undergo MRI. All patients underwent a standardized research exam at the UCSD NAFLD research center clinic with additional detail provided in the supplemental material.

Primary and Secondary Outcome

The primary outcome was the CAP detection of HIV-associated NAFLD based on MRI-PDFF ≥ 5% after exclusion of other causes of liver disease (as described above). The secondary outcome was the CAP detection of moderate-to-severe liver fat defined as MRI-PDFF ≥ 10%.

Ultrasound-based Assessment

CAP was measured simultaneously with LS by an experienced operator using the 502 Touch model (M Probe, XL Probe; Echosens, Paris, France) of the FibroScan device [23]. Measurements were obtained with the patient in the supine position with the right arm fully adducted and with the probe placed in a right intercostal space overlying the right lobe of the liver during a 10-second breath hold. The measurement was obtained after at least a three hour fast and included a minimum of 10 valid measurements. All patients were initially scanned with the M probe and when indicated by the equipment on initial assessment rescanned with the XL probe, which has been shown to reduce the failure rate of Fibroscan in obese patients. The automatic probe selection software included in the device recommends use of the XL probe when the skin to liver capsule distance is >25 mm. An unreliable LS was defined as <10 valid measurements and/or IQR/median >30% [24]. The CAP value, a marker of the attenuation of ultrasound waves in dB/m, was automatically measured simultaneously in the same region of interest as the valid LS [25]. CAP is evaluated using the same radio-frequency data as the LS and is only reported if the LS measurement is valid.

MRI-PDFF for Liver Fat Quantification

MRI was performed at the UCSD MR3T Research Laboratory using the 3T research scanner (GE Signa EXCITE HDxt; GE Healthcare, Waukesha, WI, USA) with all participants in the supine position. MRI-PDFF was used as a marker of liver fat. The details of the MRI protocol have been previously described [16, 26] and are included in the supplemental material.

Statistical Analyses

Given previous data on the diagnostic accuracy of CAP for liver fat using MRI-PDFF as the reference standard in primary

NAFLD [25], we estimated a diagnostic accuracy of 0.80 and correlation between MRI-PDFF and CAP of 0.60, which would require a sample size of 38 with a power of 0.80 and alpha of 0.05 assuming that 80% of patients had HIV-associated NAFLD. Demographic, anthropometric, laboratory, and imaging data were summarized using the mean and standard deviation for continuous variables or median and interquartile range (IQR) as appropriate. A *t*-test was performed on continuous variables with normal distribution and Kruskall-Wallis test performed on other continuous variables. The χ^2 or Fisher exact test was performed on categorical variables. Receiver operating characteristic (ROC) curve analysis was used to assess the diagnostic accuracy of CAP for the presence of HIV-associated NAFLD (MRI-PDFF ≥ 5%) and the presence of moderate to severe steatosis (MRI-PDFF ≥ 10%). For the primary and secondary outcomes, the area under the ROC curve (AUROC), optimal thresholds, sensitivity, specificity, positive predictive value (PPV), and negative predictive value (NPV) were reported. Exploratory analyses were performed to evaluate if the diagnostic accuracy of CAP varied by the presence of obesity, the probe used, or elevated IQR of the CAP measurement.

RESULTS

Baseline Characteristics

Eighty-seven patients were screened, and 70 PLWH were included in this study (Supplemental Figure 1). The study population was predominantly male (N = 63, 90%) with a mean (± standard deviation [SD]) age of 48.6 (±10.2) years and BMI of 30 (± 5.3) kg/m^2, respectively. Most participants in our cohort had a well-controlled HIV infection, the median (IQR) CD4 count was 696 (415) cells/mm^3. The most common antiretroviral regimens was composed of 2 NNRTI and 1 NRRTI followed by 2 NRTI and INSIT and 2 NRTI and a boosted PI. The prevalence of HIV-associated NAFLD (MRI-PDFF ≥ 5%) was 80% (N = 63), and 53% (N = 37) had liver fat on MRI-PDFF ≥ 10% consistent with moderate to severe steatosis (Table 1). Thirty patients had elevated liver stiffness measurement (LSM) on VCTE (> 6.2 kPa), and 3 patients had LSM associated with cirrhosis (>11.8 kPa). The M and XL probes were used for 56% and 44% of patients respectively. The mean time between CAP and MRI-PDFF was 7.5 (± 12.3 SD) days. In 15% (N = 10) patients the percentage of valid to total measurements was <60%. There were no adverse events associated with MRI or CAP. Higher BMI, ALT, AST, triglycerides, glucose, HOMA-IR, hemoglobin A1C, and dyslipidemia were associated with increasing liver fat on MRI-PDFF. CAP measurements significantly increased with increasing liver fat on MRI-PDFF, r = 0.6429, $P < .001$ (Figure 1).

Diagnostic Accuracy of CAP for HIV-associated NAFLD

The AUROC c-statistic of CAP for the detection of HIV-associated NAFLD was 0.82 (95% confidence interval [CI]: .69–.95) (Figure 2*A*). The optimal cut-point, maximizing sensitivity, and specificity, was 285 dB/m. The sensitivity, specificity, PPV, and NPV were 73.2%, 78.6%, 93.2%, and 42.3%, respectively (Table 2).

Diagnostic Accuracy of CAP for MRI-PDFF ≥ 10%

The AUROC c-statistic of CAP for the detection of moderate to severe liver fat (MRI-PDFF ≥ 10%) was 0.83 (95% CI: .72–.93) (Figure 2*B*). The optimal cut-point, maximizing sensitivity and specificity, was 314 dB/m. The sensitivity, specificity, PPV, and NPV were 78.4%, 81.8%, 82.9%, and 77.1%, respectively (Table 2).

Sensitivity Analyses for the Performance of CAP

When stratified by the IQR of CAP, we observed that an IQR below 30 dB/m was associated with a nonsignificant increase in diagnostic accuracy versus those with an IQR above 30 dB/m (AUROC c-statistic: 0.87 [95% CI, .57–1.00] vs 0.82 [95% CI, .65–.99]; $P = .97$), but the study lacked the power to detect a differences between these IQR strata. Furthermore, the results remained statistically significant even after adjustment for BMI. BMI did not affect the diagnostic accuracy of CAP (AUROC c-statistic: 0.76 [95% CI, .59–.94] for BMI < 30 kg/m^2 vs 0.91 [95% CI, .80–1.00] for BMI ≥ 30 kg/m^2; $P = .1701$). The diagnostic accuracy was similar with M and XL probes (AUROC c-statistic: 0.83 [95% CI, .68–.98] for the M probe vs 0.73 [95% CI, .38–1.00] for the XL probe; $P = .6042$).

DISCUSSION

Using a well-characterized cohort of PLWH at risk for HIV-associated NAFLD, this study determined an optimal threshold for CAP for the detection of HIV-associated NAFLD at 285 dB/m, with good diagnostic accuracy (AUROC 0.82, 95% CI, .69–.95) and excellent positive predictive value of 93.2%. This optimal threshold of 285 dB/m is similar to the optimal threshold in primary NAFLD (288 dB/m) and differs from the cut-point of 238 dB/m, which has been utilized in multiple previous studies of HIV-associated NAFLD [21]. Furthermore, a threshold of 314 dB/m can be used to detect moderate to severe liver fat, and CAP was not affected by the presence of obesity.

To date, disease-specific thresholds for CAP in HIV-associated NAFLD have not been prospectively validated with MRI-PDFF as the reference. An optimal threshold in this population should be both sensitive and specific for diagnosis of elevated liver fat (MRI-PDFF >5%) to allow early identification of patients who may benefit from interventions. Prior studies of PLWH have utilized a cut-point of 238 dB/m, which was not derived in a population of patients at risk for HIV-associated NAFLD and has subsequently demonstrated poor correlation with more accurate methods of quantifying liver fat including MR spectroscopy and MRI-PDFF [21, 27–30]. More recent studies have adopted a cut-point of 248 dB/m, which was derived from a meta-analysis published in 2017, which included diverse causes of liver disease among whom 7% had NAFLD [31–35]. A recent open-label, multicenter, randomized study that assessed

Table 1. Study Characteristics Stratified by Liver Fat

	MRI-PDFF < 5% (n = 14)	MRI-PDFF 5–10% (n = 19)	MRI-PDFF > 10% (n = 37)	*P*-Value
Demographics				
Age (years)	51.4 ± 8.7	49.6 ± 11.3	47.1 ± 10.2	.3682
Male patients	11 (78.6%)	17 (89.5%)	35 (94.6%)	.2411
White (vs. non)	5 (35.7%)	7 (36.8%)	11 (29.7%)	.8384
Hispanic (vs. non)	7 (50.0%)	11 (57.9%)	26 (70.3%)	.3565
Clinical				
Weight (kg)	79.2 ± 11.0	91.7 ± 16.6	92.1 ± 16.8	**.0316**
Height (m)	172.1 ± 9.4	172.8 ± 9	172.1 ± 7.3	.9497
BMI (kg/m^2)	26.9 ± 4.6	30.9 ± 4.7	30.7 ± 4.5	**.0245**
BMI ≥ 30	2 (14.3%)	8 (44.4%)	19 (52.8%)	**.0465**
Diabetes	0	2 (10.5%)	9 (24.3%)	.0856
Biochemical profile				
ALT (IU/L)	30.5 (19)	46 (34)	73 (61)	**< .0001**
AST (IU/L)	24.5 (20)	29 (29)	39 (30)	**.0311**
AST:ALT	0.9 (0.8)	0.7 (0.4)	0.6 (0.2)	**< .0001**
Alk phos (U/L)	67 (17)	95 (28)	74 (36)	**.0105**
Total bilirubin (mg/dL)	0.5 (0.3)	0.5 (0.4)	0.5 (0.3)	.7889
Protime (s)	11.5 (0.8)	11.2 (0.8)	11.3 (0.8)	.3500
Triglycerides (mg/dL)	116.5 (48)	159 (95)	178 (117)	**.0191**
Total cholesterol (mg/dL)	193.5 (30)	169 (55)	179 (49)	.4534
LDL (mg/dL)	115.5 (31)	93 (25)	106 (44)	.2569
FFA (mmol/L)	0.5 (0.3)	0.7 (0.4)	0.5 (0.2)	.3189
Glucose (mg/dL)	94 (15)	108 (45)	101 (18)	**.0247**
Insulin (μU/mL)	15.5 (13)	25 (25)	30 (22)	.0926
HOMA-IR	3.3 (3.1)	6.8 (6.8)	7.5 (6)	**.0182**
Hgb A1C (%)	5.2 (0.5)	5.4 (0.5)	5.6 (0.9)	**.0017**
CD4 count	791 (688)	680 (457)	638 (363)	.9544
Imaging				
MRI-PDFF	2.7 (1.6)	7 (2)	16.5 (9.3)	**< .0001**
VCTE (kPa)				
Median	5.3 (2.2)	6.7 (3.1)	5.9 (3.7)	.1788
IQR	0.8 (0.6)	0.7 (1)	0.8 (0.9)	.4132
IQR/M	15 (10)	11 (11)	13 (11)	.2585
Success rate <60%, n (%)	2 (14.3%)	4 (21.1%)	4 (10.8%)	.5423
CAP (dB/m)				
Median	246 (70)	281 (93)	343 (47)	**< .0001**
IQR	37 (10)	28 (31)	32 (17)	.4576
Probe size, n (%)				.3351
Medium	10 (71.4%)	11 (57.9%)	18 (48.7%)	.3351
XL	4 (28.6%)	8 (42.1%)	19 (51.4%)	
Metabolic Factors, n (%)				
Waist >102 cm men, > 88 cm women	6 (42.9%)	10 (52.3%)	21 (58.3%)	.6123
Triglycerides ≥ 150 mg/dL	3 (21.4%)	10 (52.6%)	24 (64.9%)	**.0214**
HDL < 40 mg/dL men, < 50 mg/dl women	1 (7.1%)	7 (36.8%)	18 51.4%)	**.0156**
SBP ≥ 130 and/or DBP ≥ 85	8 (57.1%)	10 (52.6%)	16 (44.4%)	.6810
FPG ≥ 100 mg/dL	4 (28.6%)	11 (57.9%)	19 (51.4%)	.2212
Metabolic Syndrome	2 (14.3%)	8 (42.1%)	18 (52.9%)	**.0475**

Data presented as mean ± SD, median (IQR), or n (%) as appropriate. *T*-test performed on continuous variables presented as mean ± SD; Kruskall-Wallis performed on all other continuous/ordinal variables. χ^2 or Fisher's exact test as appropriate on all categorical variables. Success rate was defined as the ratio of the number of valid measurements to the total number of measurements.

Abbreviations: ALK phos, alkaline phosphatase; ALT, alanine aminotransferase; AST, aspartate aminotransferase; BMI, body mass index; CRP, C-reactive protein; FFA, free fatty acids; GGT, gamma-glutamyl transferase; Hgb A1C, hemoglobin A1C; HDL, high-density lipoprotein; HOMA, homeostatic model assessment; IQR, interquartile range; LDL, low-density lipoprotein; MRI-PDFF, magnetic resonance imaging proton-density fat fraction; VCTE, vibration-controlled transient elastography.

the impact on liver steatosis over 48 weeks of switching from efavirenz to raltegravir while maintaining a stable NRTI backbone highlights the need for CAP standardization in PLWH [36]. The study found that the median difference in CAP values between baseline and week 48 was a decrease of 20 dB/m for people on raltegravir compared to an increase of 30 dB/m for

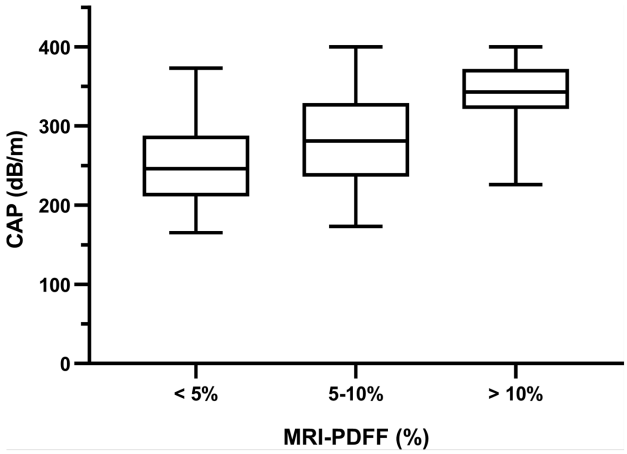

Figure 1. Distribution of CAP measurements by liver fat content on MRI-PDFF. CAP measurements increase with increasing liver fat content on MRI-PDFF, $P < .0001$. Abbreviations: CAP, controlled attenuation parameter; MRI-PDFF, magnetic resonance imaging proton-density fat fraction.

those on efavirenz. However, the study utilized a cut-point of ≥ 238 dB/m for the diagnosis of HIV-associated NAFLD. The median values used for study inclusion criteria may have included many patients without HIV-associated NAFLD, which could impact the clinical significance of the findings. Furthermore, the study included patients with HIV-HCV coinfection, which may have affected the appropriate CAP cut-point. A more recent study by Lemoine and colleagues reported an optimal cut-point of 280 dB/m for the diagnosis of moderate to severe steatosis on liver biopsy in PLWH [37]. However, the cut-point in this study grouped PLWH with mild steatosis together with those with no steatosis and did not evaluate the diagnostic accuracy of CAP with MRI-PDFF as the reference. MRI-PDFF provides a quantitative, accurate, continuous measure of liver fat compared to broad categorical classifications, which grade hepatic steatosis on liver biopsy. Furthermore, the Lemoine study did not include the use of the XL probe which was used in 44% of patients in this study population. Our study validated the CAP cut-point for primary NAFLD in PLWH and included the use of both M and XL probes making it the most representative of current clinical practice. A recent study of patients with primary NAFLD with liver biopsy as the referent found an optimal cut-point of 302 dB/m for ≥ 5% steatosis, but only 4% of patients in that study had normal liver histology, and the high prevalence of moderate-to-severe steatosis may have right-shifted the optimal cut-point [38]. Studies in primary NAFLD with M versus XL probe have demonstrated that CAP measurements are higher when using the XL probe, and the use of the XL probe in obese patients decreases the risk of Fibroscan failure [21, 39–41]. Importantly, Caussy and colleagues evaluated the diagnostic accuracy of CAP for the diagnosis of primary NAFLD using MRI-PDFF as the reference standard and found a similar optimal threshold (288 dB/m) and good diagnostic accuracy [33].

CAP performance for the diagnosis of moderate to severe steatosis defined as MRI-PDFF ≥ 10% remained good with a c-statistic of 0.83, sensitivity 78.4%, specificity 81.8%, NPV 77.1%, and PPW 82.9%. This higher cut-point may be utilized to identify PLWH with high liver-fat who may benefit from clinical trials of emerging treatments with an antisteatotic mechanism of action. Furthermore, the presence of obesity did not

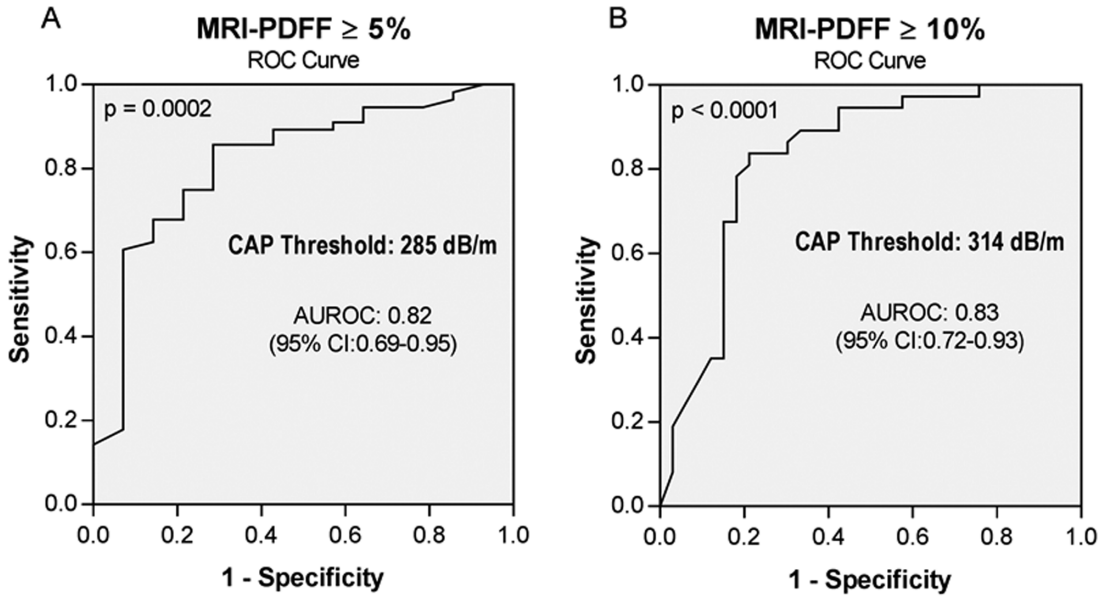

Figure 2. Diagnostic accuracy of CAP for the detection of elevated liver fat on MRI-PDFF. *A*, MRI-PDFF ≥ 5%. *B*, MRI-PDFF ≥ 10%. Abbreviations: AUROC, area under the ROC curve; CAP, controlled attenuation parameter; CI, confidence interval; MRI-PDFF, magnetic resonance imaging proton-density fat fraction; ROC, receiver operating characteristic.

Table 2. Diagnostic Accuracy of CAP for the Detection of Liver Fat

	AUROC (95% CI)	Cutoff (dB/m)	Sensitivity (%)	Specificity (%)	PPV (%)	NPV (%)
Primary analysis: MRI-PDFF ≥ 5%						
CAP (dB/m)	0.82 (.69–.95)	285	73.2	78.6	93.2	42.3
Secondary analysis: MRI-PDFF ≥ 10%						
CAP (dB/m)	0.83 (.72–.93)	314	78.4	81.8	82.9	77.1

Abbreviations: AUROC, area under the ROC curve; CAP, controlled attenuation parameter; CI, confidence interval; MRI-PDFF, magnetic resonance imaging proton-density fat fraction; NPV, negative predictive value; PPV, positive predictive value.

affect the diagnostic accuracy of CAP in our study. Although studies in primary NAFLD demonstrated higher diagnostic accuracy when the IQR of CAP measurements is < 30 dB/m, our study did not demonstrate a significant difference in PLWH but may have been underpowered for this sensitivity analysis.

As clinics treating PLWH may now have access to Fibroscan, CAP can provide an accessible, reliable tool to identify patients with elevated liver fat. Furthermore, CAP may serve as an important screening tool for potential candidates for clinical trials of pharmacologic agents for the treatment of HIV-associated NAFLD. A cut-point established using MRI-PDFF as the reference standard is relevant as liver fat quantified by MRI was the primary endpoint in both recent trials of HIV-associated NAFLD [42, 43]. Aramchol, an oral stearoyl-coenzyme-A-desaturase-1 inhibitor, which demonstrated efficacy in primary NAFLD was evaluated in a clinical trial of HIV-associated NAFLD and did not demonstrate efficacy in reducing liver fat measured by MRI-PDFF in HIV-associated NAFLD [42]. However, a randomized double-blinded multicenter study demonstrated that tesamorelin was more effective than placebo at reducing liver fat in patients with HIV-associated NAFLD [43].

We acknowledge that the study does have limitations, including that it was a single-center study at a tertiary care center and included predominantly male patients. HIV-associated NAFLD was highly prevalent due to the study criteria requiring the presence of metabolic risk factors, which may affect generalizability; however, the study population reflects a high-risk population, which has the greatest likelihood of benefitting from systematic screening. Furthermore, the prevalence of fibrosis, obesity and other metabolic risk factors may affect the optimal cut-point in our study, however, our results were similar to recently published work of primary NAFLD. In addition, we did not acquire reproducibility data of CAP, however this has been performed in large cohorts of patients with primary NAFLD [40]. Our study had limited power to assess for differences in diagnostic accuracy associated with IQR of CAP > 30 dB/m and with increasing liver fibrosis. Finally, this study did not include liver histology. However, to determine the diagnostic accuracy of CAP, patients with nonpathologic levels of liver fat must be included, and it would be unethical to subject these patients to a liver biopsy. Furthermore, MRI-PDFF is a quantitative reference standard, which provides a detailed, accurate, reproducible assessment of liver fat from all segments of the liver and across the full range of physiologic liver fat content, whereas liver histology has suboptimal inter- and intra-observer agreement in NAFLD [10, 16, 44, 45].

In a prospective sample of PLWH at risk for HIV-associated NAFLD we demonstrated good diagnostic accuracy and excellent positive predictive value for CAP for detection of NAFLD (MRI-PDFF ≥ 5%). The results of this provide a disease-specific threshold value that could be used to rule in NAFLD in future studies of PLWH at risk for HIV-associated NAFLD. As newer trials for patients with HIV-associated NAFLD emerge, accessible screening tools, including CAP with clearly defined cut-points, will be critical to identify patients who may qualify for clinical trials without a high burden of false-positive results and screen failures. Furthermore, the use of this disease-specific threshold that can be obtained concomitantly with LS measurement can help identify PLWH who may benefit from subspecialty hepatology referral. In addition, recent studies in primary NAFLD suggest that in early stages of the disease, the degree of steatosis may predict early disease progression, although this observation will require further validation [46]. Future studies evaluating the optimal strategy and cost-effectiveness of screening PLWH for HIV-associated NAFLD are needed.

Supplementary Data

Supplementary materials are available at *Clinical Infectious Diseases* online. Consisting of data provided by the authors to benefit the reader, the posted materials are not copyedited and are the sole responsibility of the authors, so questions or comments should be addressed to the corresponding author.

Notes

Author contributions. V. A.: analysis and interpretation of data, drafting of the manuscript, critical revision of the manuscript, approved final submission.

E. C.: patient recruitment, critical revision of the manuscript, approved final submission.

C. R.: patient recruitment, critical revision of the manuscript, approved final submission.

S. B.: data collection, critical revision of the manuscript, approved final submission.

S. S.: data collection, critical revision of the manuscript, approved final submission.

R. B.: data analysis, critical revision of the manuscript, approved final submission.

L. R.: patient visits, critical revision of the manuscript, approved final submission.

G. H.: data analysis, critical revision of the manuscript, approved final submission.

M. M.: data analysis, critical revision of the manuscript, approved final submission.

K. F.: data analysis, critical revision of the manuscript, approved final submission.

C. S.: data analysis, critical revision of the manuscript, approved final submission.

R. L.: study concept and design, analysis and interpretation of data, drafting of the manuscript, critical revision of the manuscript, obtained funding, study supervision, approved final submission.

Acknowledgments. The authors acknowledge the patients who contributed to this study.

Disclaimer. The content is solely the responsibility of the authors and does not necessarily represent the official views of the National Institutes of Health.

Financial support. Supported by an investigator initiated study grant to R. L. by Galmed. R. L. receives funding support from National Institute of Environmental Health Sciences (5P42ES010337), National Center for Advancing Translational Sciences (5UL1TR001442), National Institute of Diabetes and Digestive and Kidney Diseases (R01DK106419, P30DK120515), (1R01DK121378), (P30DK120515), and Department of Defense, Peer Reviewed Cancer Research Program (CA170674P2). V. A. is supported by the NIDDK K23- DK119460.

Potential conflicts of interests. K. F. serves as representative of UC Regents for GE Healthcare, Bayer, AMRA, Fulcrum Therapeutics, IBM/Watson Health, and Epigenomics; Advisory Board as representative of UC Regents for AMRA, Guerbet, and Bristol Myers Squibb; grants from Gilead, GE Healthcare, Siemens, GE MRI, Bayer, GE Digital, GE US, ACR Innovation, Philips, Celgene; lab service agreements with Enanta, ICON Medical Imaging, Gilead, Shire, Virtualscopics, Intercept, Synageva, Takeda, Genzyme, Janssen, NuSirt, Celgene-Parexel, and Organovo. E. C. receives unrelated grants from Gilead and Merck, and personal fees from Gilead. R. L. serves as a consultant or advisory board member for Arrowhead Pharmaceuticals, AstraZeneca, Bird Rock Bio, Boehringer Ingelheim, Bristol-Myer Squibb, Celgene, Cirius, CohBar, Conatus, Eli Lilly, Enanta, Galmed, Gemphire, Gilead, Glympse bio, GNI, GRI Bio, Intercept, Ionis, Janssen Inc., Madrigal, Merck, Metacrine, Inc., NGM Biopharmaceuticals, Novartis, Novo Nordisk, Pfizer, Prometheus, Receptos, Sanofi, Siemens, and Viking Therapeutics. In addition, his institution has received grant support from Allergan, Boehringer-Ingelheim, Bristol-Myers Squibb, Cirius, Daiichi-Sankyo Inc., Eli Lilly and Company, Galectin Therapeutics, Galmed Pharmaceuticals, GE, Genfit, Gilead, Intercept, Grail, Janssen, Madrigal Pharmaceuticals, Merck, NGM Biopharmaceuticals, NuSirt, Pfizer, pH Pharma, Prometheus, Sirius, and Siemens. He is also cofounder of Liponexus, Inc. C. R. receives grants from Gilead and Abbvie, and personal fees from Gilead, Abbvie, Viiv, and Merck. M. M. serves as a consultant for Arrowhead, Glympse, Kowa, Median, and Novo Nordisk. In addition, his institution has received laboratory service agreement support from Alexion, AstraZeneca, Bristol-Myers Squibb, Celgene, Enanta, Galmed, Genzyme, Gilead, Guerbet, Intercept, Ionis, Isis, Janssen, NuSirt, Organovo, Pfizer, Roche, Sanofi, Shire, Synageva, and Takeda and grant support from Guerbet; and is a stockholder in General Electric and Pfizer. C. S. serves as consultant to Blade, Epigenomics, and Boehinger. He is or was the representative on an institutional consultation agreement from IBM-Watson, AMRA, BMS, Exact Sciences, and GE Digital. He is or was a principal investigator on grants from Bayer, GE, Foundation of NIH, Gilead, and Philips, and Siemens. In addition, his institution has received support through laboratory services agreements with Alexion, AstraZeneca, Bristol-Myers Squibb, Celgene, Enanta, Galmed, Genzyme, Gilead, ICON, Intercept, Isis, Janssen, NuSirt, Pfizer, Roche, Sanofi, Shire, Synageva, and Takeda. He also reports educational materials royalties from Wolters Kluwer. All other authors report no potential conflicts. All authors have submitted the ICMJE Form for Disclosure of Potential Conflicts of Interest. Conflicts that the editors consider relevant to the content of the manuscript have been disclosed.

References

1. Weber R, Sabin CA, Friis-Møller N, et al. Liver-related deaths in persons infected with the human immunodeficiency virus: the D:A:D study. Arch Intern Med **2006**; 166:1632–41.
2. Nguyen KA, Peer N, Mills EJ, Kengne AP. A meta-analysis of the metabolic syndrome prevalence in the global HIV-infected population. PLoS One **2016**; 11:e0150970.
3. van Zoest RA, Wit FW, Kooij KW, et al; AGEhIV Cohort Study Group. Higher prevalence of hypertension in HIV-1-infected patients on combination antiretroviral therapy is associated with changes in body composition and prior stavudine exposure. Clin Infect Dis **2016**; 63:205–13.
4. Levy ME, Greenberg AE, Hart R, Powers Happ L, Hadigan C, Castel A; DC Cohort Executive Committee. High burden of metabolic comorbidities in a city-wide cohort of HIV outpatients: evolving health care needs of people aging with HIV in Washington, DC. HIV Med **2017**; 18:724–35.
5. Mohammed SS, Aghdassi E, Salit IE, et al. HIV-positive patients with nonalcoholic fatty liver disease have a lower body mass index and are more physically active than HIV-negative patients. J Acquir Immune Defic Syndr **2007**; 45:432–8.
6. Dinh DM, Volpe GE, Duffalo C, et al. Intestinal microbiota, microbial translocation, and systemic inflammation in chronic HIV infection. J Infect Dis **2015**; 211:19–27.
7. Price JC, Seaberg EC, Latanich R, et al. Risk factors for fatty liver in the Multicenter AIDS Cohort Study. Am J Gastroenterol **2014**; 109:695–704.
8. Hernaez R, Lazo M, Bonekamp S, et al. Diagnostic accuracy and reliability of ultrasonography for the detection of fatty liver: a meta-analysis. Hepatology **2011**; 54:1082–90.
9. Zhang Y, Wang C, Duanmu Y, et al. Comparison of CT and magnetic resonance mDIXON-Quant sequence in the diagnosis of mild hepatic steatosis. Br J Radiol **2018**; 91:20170587.
10. Reeder SB, Cruite I, Hamilton G, Sirlin CB. Quantitative assessment of liver fat with magnetic resonance imaging and spectroscopy. J Magn Reson Imaging **2011**; 34:729–49.
11. Asrani SK. Incorporation of noninvasive measures of liver fibrosis into clinical practice: diagnosis and prognosis. Clin Gastroenterol Hepatol **2015**; 13:2190–204.
12. Doycheva I, Cui J, Nguyen P, et al. Non-invasive screening of diabetics in primary care for NAFLD and advanced fibrosis by MRI and MRE. Aliment Pharmacol Ther **2016**; 43:83–95.
13. Dulai PS, Sirlin CB, Loomba R. MRI and MRE for non-invasive quantitative assessment of hepatic steatosis and fibrosis in NAFLD and NASH: clinical trials to clinical practice. J Hepatol **2016**; 65:1006–16.
14. Loomba R, Sirlin CB, Ang B, et al; San Diego Integrated NAFLD Research Consortium (SINC). Ezetimibe for the treatment of nonalcoholic steatohepatitis: assessment by novel magnetic resonance imaging and magnetic resonance elastography in a randomized trial (MOZART trial). Hepatology **2015**; 61:1239–50.
15. Idilman IS, Keskin O, Celik A, et al. A comparison of liver fat content as determined by magnetic resonance imaging-proton density fat fraction and MRS versus liver histology in non-alcoholic fatty liver disease. Acta Radiol **2016**; 57:271–8.
16. Permutt Z, Le TA, Peterson MR, et al. Correlation between liver histology and novel magnetic resonance imaging in adult patients with non-alcoholic fatty liver disease - MRI accurately quantifies hepatic steatosis in NAFLD. Aliment Pharmacol Ther **2012**; 36:22–9.
17. Tang A, Desai A, Hamilton G, et al. Accuracy of MR imaging-estimated proton density fat fraction for classification of dichotomized histologic steatosis grades in nonalcoholic fatty liver disease. Radiology **2015**; 274:416–25.
18. Park CC, Nguyen P, Hernandez C, et al. Magnetic resonance elastography vs transient elastography in detection of fibrosis and noninvasive measurement of steatosis in patients with biopsy-proven nonalcoholic fatty liver disease. Gastroenterology **2017**; 152:598–607.e2.
19. Noureddin M, Lam J, Peterson MR, et al. Utility of magnetic resonance imaging versus histology for quantifying changes in liver fat in nonalcoholic fatty liver disease trials. Hepatology **2013**; 58:1930–40.
20. Sasso M, Beaugrand M, de Ledinghen V, et al. Controlled attenuation parameter (CAP): a novel VCTE™ guided ultrasonic attenuation measurement for the evaluation of hepatic steatosis: preliminary study and validation in a cohort of patients with chronic liver disease from various causes. Ultrasound Med Biol **2010**; 36:1825–35.
21. Caussy C, Alquiraish MH, Nguyen P, Hernandez C, Cepin S, Fortney LE, Ajmera V, et al. Optimal threshold of controlled attenuation parameter with MRI-PDFF as the gold standard for the detection of hepatic steatosis. Hepatology **2018**; 67:1348–59.

22. Classification and diagnosis of diabetes: standards of medical care in diabetes-2018. Diabetes Care **2018**;41:S13–27.
23. Sandrin L, Fourquet B, Hasquenoph JM, et al. Transient elastography: a new noninvasive method for assessment of hepatic fibrosis. Ultrasound Med Biol **2003**; 29:1705–13.
24. Castera L, Forns X, Alberti A. Non-invasive evaluation of liver fibrosis using transient elastography. J Hepatol **2008**; 48:835–47.
25. Caussy C, Alquiraish MH, Nguyen P, et al. Optimal threshold of controlled attenuation parameter with MRI-PDFF as the gold standard for the detection of hepatic steatosis. Hepatology **2018**; 67:1348–59.
26. Patel NS, Peterson MR, Brenner DA, Heba E, Sirlin C, Loomba R. Association between novel MRI-estimated pancreatic fat and liver histology-determined steatosis and fibrosis in non-alcoholic fatty liver disease. Aliment Pharmacol Ther **2013**; 37:630–9.
27. Price JC, Dodge JL, Ma Y, et al. Controlled attenuation parameter and magnetic resonance spectroscopy-measured liver steatosis are discordant in obese HIV-infected adults. AIDS **2017**; 31:2119–25.
28. Sasso M, Miette V, Sandrin L, Beaugrand M. The controlled attenuation parameter (CAP): a novel tool for the non-invasive evaluation of steatosis using Fibroscan. Clin Res Hepatol Gastroenterol **2012**; 36:13–20.
29. Sulyok M, Makara M, Rupnik Z, et al. Hepatic steatosis in individuals living with HIV measured by controlled attenuation parameter: a cross-sectional study. Eur J Gastroenterol Hepatol **2015**; 27:679–85.
30. Vuille-Lessard É, Lebouché B, Lennox L, et al. Nonalcoholic fatty liver disease diagnosed by transient elastography with controlled attenuation parameter in unselected HIV monoinfected patients. AIDS **2016**; 30:2635–43.
31. Karlas T, Petroff D, Sasso M, et al. Individual patient data meta-analysis of controlled attenuation parameter (CAP) technology for assessing steatosis. J Hepatol **2017**; 66:1022–30.
32. Aepfelbacher JA, Balmaceda J, Purdy J, et al. Increased prevalence of hepatic steatosis in young adults with lifelong HIV. J Infect Dis **2019**; 220:266–9.
33. Sebastiani G, Saeed S, Lebouche B, et al; LIVEHIV Study Group. Vitamin E is an effective treatment for nonalcoholic steatohepatitis in HIV mono-infected patients. AIDS **2020**; 34:237–44.
34. Perazzo H, Cardoso SW, Yanavich C, et al. Predictive factors associated with liver fibrosis and steatosis by transient elastography in patients with HIV mono-infection under long-term combined antiretroviral therapy. J Int AIDS Soc **2018**; 21:e25201.
35. Pembroke T, Deschenes M, Lebouché B, et al. Hepatic steatosis progresses faster in HIV mono-infected than HIV/HCV co-infected patients and is associated with liver fibrosis. J Hepatol **2017**; 67:801–8.
36. Macías J, Mancebo M, Merino D, et al; Spanish AIDS Research Network-HEP09 Study Group. Changes in liver steatosis after switching from efavirenz to raltegravir among human immunodeficiency virus-infected patients with nonalcoholic fatty liver disease. Clin Infect Dis **2017**; 65:1012–9.
37. Lemoine M, Assoumou L, De Wit S, et al; ANRS-ECHAM Group. Diagnostic accuracy of noninvasive markers of steatosis, nash, and liver fibrosis in HIV-monoinfected individuals at risk of Nonalcoholic Fatty Liver Disease (NAFLD): results from the ECHAM study. J Acquir Immune Defic Syndr **2019**; 80:e86–94.
38. Eddowes PJ, Sasso M, Allison M, et al. Accuracy of fibroscan controlled attenuation parameter and liver stiffness measurement in assessing steatosis and fibrosis in patients with nonalcoholic fatty liver disease. Gastroenterology **2019**; 156:1717–30.
39. Chan WK, Nik Mustapha NR, Wong GL, Wong VW, Mahadeva S. Controlled attenuation parameter using the FibroScan® XL probe for quantification of hepatic steatosis for non-alcoholic fatty liver disease in an Asian population. United European Gastroenterol J **2017**; 5:76–85.
40. Vuppalanchi R, Siddiqui MS, Van Natta ML, et al; NASH Clinical Research Network. Performance characteristics of vibration-controlled transient elastography for evaluation of nonalcoholic fatty liver disease. Hepatology **2018**; 67:134–44.
41. de Lédinghen V, Hiriart JB, Vergniol J, Merrouche W, Bedossa P, Paradis V. Controlled attenuation parameter (CAP) with the XL probe of the Fibroscan®: a comparative study with the M probe and liver biopsy. Dig Dis Sci **2017**; 62:2569–77.
42. Ajmera VH, Cachay E, Ramers C, et al. MRI assessment of treatment response in HIV-associated NAFLD: a randomized trial of a stearoyl-coenzyme-a-desaturase-1 inhibitor (ARRIVE Trial). Hepatology **2019**; 70:1531–45.
43. Stanley TL, Fourman LT, Feldpausch MN, et al. Effects of tesamorelin on non-alcoholic fatty liver disease in HIV: a randomised, double-blind, multicentre trial. Lancet HIV **2019**; 6:e821–30.
44. Tang A, Tan J, Sun M, et al. Nonalcoholic fatty liver disease: MR imaging of liver proton density fat fraction to assess hepatic steatosis. Radiology **2013**; 267:422–31.
45. Ratziu V, Charlotte F, Heurtier A, et al; LIDO Study Group. Sampling variability of liver biopsy in nonalcoholic fatty liver disease. Gastroenterology **2005**; 128:1898–906.
46. Ajmera V, Park CC, Caussy C, et al. Magnetic resonance imaging proton density fat fraction associates with progression of fibrosis in patients with nonalcoholic fatty liver disease. Gastroenterology **2018**; 155:307–10.e2.